Mesenchymal Stem Cells Prevent Progressive Experimental Renal Failure but Maldifferentiate into Glomerular Adipocytes

Uta Kunter,* Song Rong,* Peter Boor,*† Frank Eitner,* Gerhard Müller-Newen,‡ Zivka Djuric,* Claudia R. van Roeyen,* Andrzej Konieczny,* Tammo Ostendorf,* Luigi Villa,* Maja Milovanceva-Popovska,* Dontscho Kerjaschki,§ and Jürgen Floege*

**Division of Nephrology, University Hospital RWTH Aachen, Aachen, Germany; †Department of Clinical and Experimental Pharmacotherapy, Slovak Medical University, Bratislava, Slovakia; ‡Institute of Biochemistry, University Hospital Rheinisch-Westfälische Technische Hochschule Aachen, Aachen, Germany; and §Department of Pathology, University of Vienna, Vienna, Austria*

Glomerulonephritis (GN) is a major cause of renal failure. This study sought to determine whether intrarenal injection of rat mesenchymal stem cells (MSC) can preserve renal function in a progressive rat model of GN. Early in GN (day 10), fluorescently labeled rat MSC localized to more than 70% of glomeruli, ameliorated acute renal failure, and reduced glomerular adhesions. Fifty days later, proteinuria had progressed in controls to 40 ± 25 mg/d but stayed low in MSC-treated rats (13 ± 4 mg/d; $P < 0.01$). Renal function on day 60 in the MSC group was better than in medium controls. Kidneys of the MSC group as compared with controls on day 60 contained 11% more glomeruli per 1-mm² section of cortex but also significantly more collagen types I, III, and IV and α-smooth muscle actin. Approximately 20% of the glomeruli of MSC-treated rats contained single or clusters of large adipocytes with pronounced surrounding fibrosis. Adipocytes exhibited fluorescence in their cytoplasm and/or intracellular lipid droplets. Lipid composition in these adipocytes *in vivo* mirrored that of MSC that underwent adipogenic differentiation *in vitro*. Thus, in this GN model, the early beneficial effect of MSC of preserving damaged glomeruli and maintaining renal function was offset by a long-term partial maldifferentiation of intraglomerular MSC into adipocytes accompanied by glomerular sclerosis. These data suggest that MSC treatment can be a valuable therapeutic approach only if adipogenic maldifferentiation is prevented.

J Am Soc Nephrol 18: 1754–1764, 2007. doi: 10.1681/ASN.2007010044

Mesenchymal stem cells (MSC) hold special promise for renal repair, because nephrons are largely of mesenchymal origin (1). The potential of MSC for renal repair has been shown in rodent models of acute renal failure (ARF), where the course of glycerol, cisplatin, or ischemia-reperfusion induced ARF was improved by MSC injection shortly after disease induction (2–5). In addition, we recently reported that injection of rat MSC into a renal artery can accelerate recovery from mesangiolytic damage and prevent transient ARF in rat anti-Thy1.1 glomerulonephritis (GN) (6). Anti-Thy1.1 nephritis is a model of acute mesangioproliferative glomerulonephritis and is characterized by initial mesangiolysis followed within a few days by glomerular repair *via* endothelial and mesangial cell proliferation and accumulation of mesangial matrix. We have also provided evidence that MSC likely exerted these effects in glomeruli by paracrine effects, such as the release of high amounts of vascular endothelial growth factor (VEGF) and TGF-β1 rather than by differentiation into resident glomerular cell types or monocytes/macrophages (6).

In this study, we investigated the long-term effects of MSC administration in early anti-Thy1.1 nephritis. Normally, anti-Thy1.1 nephritis in rats follows a self-limited course, and spontaneous restitution of the glomerular architecture can be observed within approximately 4 wk. For enhancement of the relevance of the model for progressive renal disease in humans, the model in this study was aggravated and transformed into a course of progressive renal failure by previous uninephrectomy of the rats (7,8).

Materials and Methods

Rats were housed under standard conditions in a light-, temperature-, and humidity-controlled environment with free access to tap water and standard rat diet. All animal protocols were approved by the local government authorities.

Harvest and Culture of MSC

Inbred male Lewis rats that weighed 180 to 210 g (Harlan, Horst, Netherlands) served as bone marrow donors; MSC were prepared as described previously (6). Cells were seeded onto six-well plates (nine

Received January 12, 2007. Accepted March 14, 2007.

Published online ahead of print. Publication date available at www.jasn.org.

U.K. and S.R. contributed equally to this work.

Address correspondence to: Dr. Uta Kunter, Division of Nephrology, University Hospital RWTH Aachen, Pauwelsstrasse 30, D-52057 Aachen, Germany. Phone: +49-241-8089670; Fax: +49-241-8082446; E-mail: utakunter@gmx.de

ISSN: 1046-6673/1806-1754

wells per donor) and cultured at 37°C in a humidified atmosphere that contained 5% CO_2. Medium was changed after 2 d and every 3 d thereafter. Nonadherent hematopoietic cells were removed when medium was changed. After a mean of 6 d, cells reached subconfluence and were detached with trypsin/EDTA, reseeded at 4×10^3 cells/cm^2, and used for experiments after the third passage.

MSC features were demonstrated by typical spindle-shaped morphology as well as osteogenic and adipogenic differentiation under appropriate *in vitro* conditions. In addition, MSC were cultured in four-well chamber slides (LAB-TEK; Nalge Nunc Int., Naperville, IL). Upon confluence in passage 3, they were washed twice with PBS, fixed in acetone for 10 min, air-dried for 30 min, and stored at −80°C until use. These slides were tested for MSC-typical presence or absence of CD antigens (CD31, CD34, CD44, CD45, CD73, and CD90).

Fluorescence Labeling for In Vivo *Tracking of Cells*

Before *in vivo* injection, cells were labeled using the PKH26 red fluorescence cell linker kit (Sigma-Aldrich, St. Louis, MO) according to the manufacturer's protocol (6). Cells were resuspended at 1×10^6 cells/250 μl complete medium and used within 30 min.

PKH 26 labeling did not affect MSC viability, because reseeding of such cells yielded >95% viable cells, which could be induced to differentiate like the unlabeled cells (data not shown). After *in vivo* experiments, PKH26-specific fluorescence was detected in frozen kidney samples as described previously (6).

Osteogenic and Adipogenic Differentiation of MSC

Osteogenic differentiation of Lewis MSC was tested following the protocol of Bruder *et al.* (US patent 5,736,396), as described previously (6). Adipogenic differentiation of MSC was tested following the protocol of M. Pittenger (US patent 5,827,740). Subconfluent MSC after the second passage were incubated in adipogenic differentiation medium (Cambrex, Charles City, IA). After 15 d, both Oil red O and Nile blue staining was performed. In addition, 1 d before and 16 d after start of adipogenic differentiation, MSC were harvested and total mRNA was extracted. Cultured rat mesangial cells that were grown in basal medium (RPMI 1640 with 10% FCS, L-glutamine, and 1% penicillin/streptomycin; all Cambrex) served as negative controls for fat cell differentiation.

Real-Time Quantitative Reverse Transcriptase–PCR

Total RNA was isolated from MSC, and real-time reverse transcriptase–PCR was performed as described previously (9). The primer sequences are listed in Table 1. Glyceraldehyde-3-phosphate dehydrogenase was used as an internal standard.

Experimental Model and Experimental Design

Inbred male Lewis rats (Harlan) that weighed 180 to 210 g were used for the experiments. One hour before disease induction, rats received a right-sided uninephrectomy *via* a lateral flank incision under isoflurane anesthesia. Anti-Thy1.1 mesangioproliferative glomerulonephritis was then induced as described previously (10). On day 2 after disease induction, either 2×10^6 MSC ($n = 10$) or an equal volume of control medium ($n = 10$) was injected intra-arterially into the left kidney as described previously (6). Five randomly selected rats in each group received an intravital renal biopsy on day 10 after disease induction (*i.e.*, on day 8 after MSC transplantation). One control rat died during this procedure from an isoflurane overdose, but none of the rats died during follow-up. Functional measurements (24-h urine collection, assessment of serum creatinine, serum urea nitrogen (SUN), and BP) were performed on days 10, 30, and 60. All rats were killed at day 60 after induction of anti-Thy1.1 nephritis, so biopsy material consisted of day 10 (five rats each) and day 60 (all rats).

Renal Morphology

Tissue for light microscopy was fixed in methyl Carnoy solution and embedded in paraffin. Four-micron sections were stained with periodic acid-Schiff (PAS) and counterstained with hematoxylin. For the evaluation of total collagen, renal tissues were stained with Sirius red. Fat cells were demonstrated in frozen kidney sections using Oil red O staining for the identification of all types of lipids and Nile blue staining for identification of neutral *versus* acidic lipids.

Immunoperoxidase Staining

Four-micrometer sections of methyl Carnoy–fixed biopsy tissue or acetone-fixed cellular monolayers that were grown on coverslips were processed by an indirect immunoperoxidase technique as described previously (10). Primary antibodies were identical to those described previously (11,12) and included murine mAb to α-smooth muscle actin (α-SMA; clone 1A4; DAKO, Carpinteria, CA) to a cytoplasmic antigen present in monocytes, macrophages, and dendritic cells (clone ED-1; Serotec, Oxford, UK) and to human muscle desmin that cross-reacts with rat desmin (clone D33; DAKO), plus goat polyclonal antibodies to human collagen types I, III, and IV (Southern Biotech, Birmingham, AL) that cross-react with rat collagen type I, III, and IV, plus appropriate negative controls using irrelevant antibodies. Primary antibodies for the characterization of cultured MSC included mouse mAb against rat CD31 (clone TLD-3A12; Serotec), rat CD34 (ICO115; Santa Cruz Biotechnology, Santa Cruz, CA), CD44 (MCA643GA; Serotec), rat CD73 (BD Pharmingen, Heidelberg, Germany), rat CD90 (clone OX7; Mediagnost, Reutlingen, Germany), and a goat polyclonal antibody against rat CD45 (M-20; Santa Cruz) plus appropriate negative controls using irrelevant antibodies.

Table 1. Primers for real- time RT-PCR [a]

Gene	Forward Primer	Reverse Primer
Adiponectin	GGGATTACTGCAACCGAAGG	CCATCCAACCTGCACAAGTTT
Leptin	TTCACACACGCAGTCGGTATC	GTGAAGCCCGGGAATGAAG
Lipoprotein lipase	GTACAGTCTTGGAGCCCATGC	GCCAGTAATTCTATTGACCTTCTTGTT
PPAR-γ	CATACATAAAGTCCTTCCCGCTG	TTGTCTGTTGTCTTTCCTGTCAAGA
GAPDH	ACAAGATGGTGAAGGTCGGTG	AGAAGGCAGCCCTGGTAACC

[a]GAPDH, glyceraldehyde-3-phosphate dehydrogenase; PPAR-γ , peroxisome proliferator–activated receptor-γ ; RT-PCR, reverse transcriptase–PCR.

Evaluation of Histologic Sections

All slides were evaluated by an observer who was unaware of their origin. In PAS-stained sections, the number of total mitotic figures within 100 to 150 glomerular cross-sections was determined as described previously (10). Mesangiolysis was graded on a semiquantitative scale (0, no mesangiolysis; 1, segmental mesangiolysis; 2, global mesangiolysis; 3, microaneurysm) as described previously (10). In addition, we counted the number of glomeruli that showed adhesions to Bowman's capsule. On day 60, the percentage of glomeruli that exhibited focal or global glomerulosclerosis was determined as described previously (13). Tubulointerstitial injury, defined as inflammatory cell infiltrates, tubular dilation, and/or atrophy or interstitial fibrosis on day 60, was graded on a scale of 0 to 4 as described previously (14). The total number of glomerular cross-sections was determined by counting within a longitudinal renal 4-μm section all glomeruli per 20 consecutive 1-mm^2 areas of the renal cortex. In sections that stained for the ED-1 antigen, total numbers of positive cells per 100 glomeruli were counted. Immunostaining for glomerular α-SMA; desmin; as well as types I, III, and IV collagen was evaluated using a point-counting method as described previously (8). Tubulointerstitial staining (Sirius red; collagen types I, III, IV; and ED-1) was evaluated by computer histomorphometry as described previously (8).

Electron Microscopy

Tissue for electron microscopy was fixed in half-strength Karnovsky solution (1% paraformaldehyde and 1.25% glutaraldehyde in 0.1 M sodium cacodylate buffer [pH 7.0]). After fixation, tissue was postfixed in 1% osmium tetroxide for 2 h, dehydrated in graded ethanols, and embedded in epoxy resin. Thin sections were stained with uranyl acetate and lead citrate and examined with a Phillips 410 (Phillips Export BV, Eindhoven, Netherlands) electron microscope. Kidney tissue examined included at least two and usually three or more glomeruli per rat as well as cortical and medullary interstitium, tubules, and blood vessels.

Miscellaneous Measurements

BP were measured by tail-cuff plethysmography on days 10, 30, and 60 in conscious rats using a programmed sphygmomanometer (BP-981; Softron, Tokyo, Japan). On days 10, 30, and 60, serum creatinine, SUN, and urinary protein excretion were measured by an autoanalyzer (Vitros 250 analyzer; Orthoclinical Diagnostics, Neckargmünd, Germany). Ratios of urinary proteinuria/urinary creatinine and creatinine clearances were calculated from 24-h urine collections.

Statistical Analyses

All values are presented as means ± SD. Statistical significance was evaluated using one-way ANOVA with modified *t* test performed with the Bonferroni correction. Repeated measurements of serum creatinine, SUN, and proteinuria were also tested using two-way repeated measures ANOVA.

Results

Characterization of Rat MSC

Lewis rat MSC exhibited spindle-shaped morphology, potential to differentiate into osteogenic and adipogenic cells (as shown previously [6]), and >95% viability after PKH26 labeling. In addition, immunocytochemical stainings for various surface markers yielded results that matched consensus criteria (15): >95% negativity for CD31, CD34, and CD45 and >95% positivity for CD73, CD44, and CD90 (Figure 1).

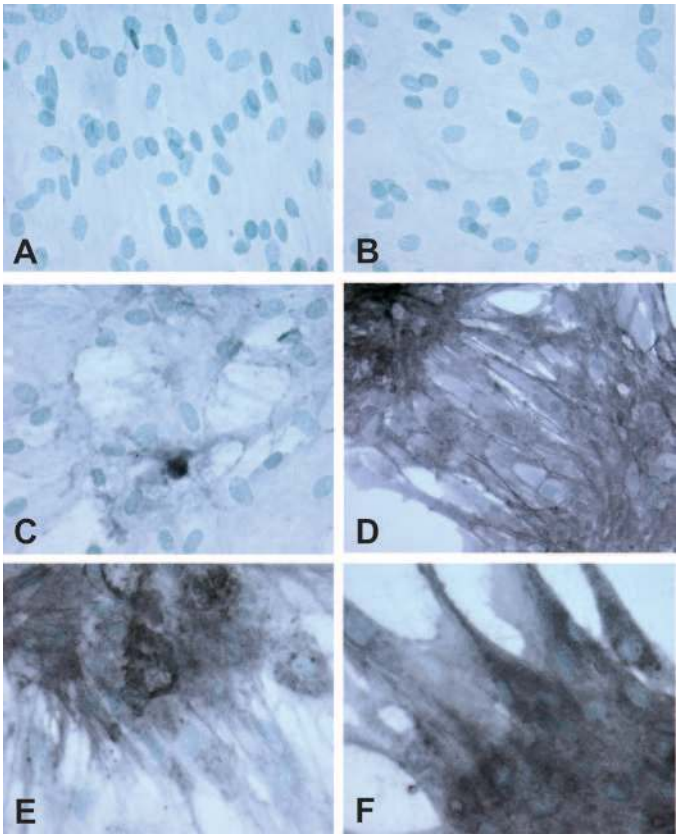

Figure 1. Expression of surface markers on mesenchymal stem cells (MSC) *in vivo* by immunocytochemistry. Lewis MSC in passage 3, grown on coverslips, show no expression of surface markers CD31 (A) and CD34 (B) and rare (<5%) expression of CD45 (C), whereas CD44 (D), CD73 (E), and CD90 (F) can be detected in >95% of the cells. Magnification, ×400.

MSC Localize to Glomeruli after Injection into the Renal Artery

Intravital biopsies that were obtained on day 10 after disease induction showed that in rats that received MSC >70% of glomeruli exhibited PKH26-specific fluorescence (Figure 2A). Most positive glomeruli contained one to three positive areas (Figure 2B). On day 60, fluorescence was not restricted to foci but distributed much more diffusely and less intensely throughout the glomeruli (Figure 2C). No PKH26-specific fluorescence was found outside glomeruli or in medium controls at any time point.

Short-Term Effects of MSC on ARF and Glomerular Morphology

In the course of anti-Thy1.1 nephritis in Lewis rats, transient ARF develops (6). In this study, the model was further aggravated by a uninephrectomy at the time point of disease induction to induce progressive renal failure.

In PAS-stained renal biopsies of day 10, ARF was evidenced by widened and flattened tubular cells and intratubular cast formation (data not shown). MSC injection significantly reduced serum creatinine and SUN, confirmed by a higher cre-

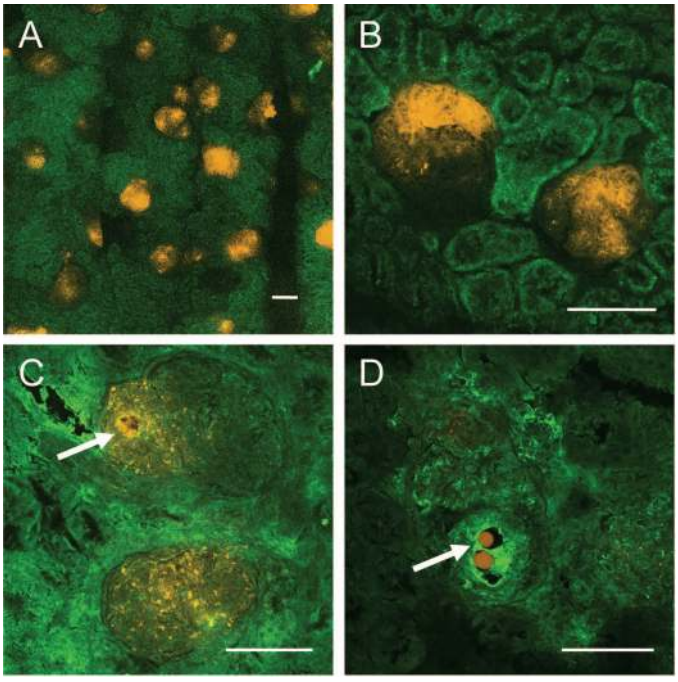

Figure 2. Laser scanning microscopy images in MSC-treated kidneys. All pictures represent overlays of channels for detection of autofluorescence (green) and detection of PKH26 (orange). (A) Frozen renal section from day 10. Focal to global accumulation of PKH26-specific fluorescence in approximately 70% of glomeruli. No extraglomerular PKH26 fluorescence. Typical bright green autofluorescence in tubular areas. (B) Detail of two glomeruli at day 10. Specific fluorescence for PKH26 is intense and mostly located to mesangial fields. (C) Late detection of fluorescence specific for PKH26. Two glomeruli from day 60. PKH26-specific fluorescence areas are located exclusively inside glomeruli with maximum intensity around a vacuolar area in the upper glomerulus (arrow). Fluorescence does not seem to be limited to specific areas/cell types (*i.e.*, mesangial fields) of the glomerulus anymore, and intensity is clearly reduced when compared with day 8. (D) Conserved lipids inside an area of suspected adipogenic differentiation with incorporation of the lipophilic dye PKH26 (arrow) on day 60. Bars = 100 μm.

atinine clearance, on day 10 when compared with medium controls but did not affect the mild proteinuria or BP (Table 2).

Both groups exhibited similar degrees of moderate, mostly focal persistent mesangiolysis on day 10 (Table 2). However, the number of glomeruli with adhesions between the glomerular tuft and Bowman's capsule was reduced by almost 50% in MSC-treated rats (Table 2). Glomerular influx of monocytes/macrophages, mitosis rates, and expression of α-SMA were not affected by MSC treatment, but the *de novo* expression of collagen type I increased significantly in the MSC group (Table 2).

MSC Reduce Proteinuria and Improve Renal Function at Follow-Up

All rats recovered from ARF by day 30, and serum creatinine and creatinine clearance values almost normalized in both groups. However, SUN remained significantly lower in MSC-*versus* medium-treated rats (Table 2). On day 60, serum creatinine started to rise again in both groups, and the difference failed to reach statistical significance ($P = 0.09$). Nevertheless, both groups showed further recovery of creatinine clearance. SUN on day 60 remained significantly lower in MSC-treated rats (Table 2). In parallel, proteinuria remained low in the MSC group on day 60, whereas it doubled in the control group between days 30 and 60 (Table 2). Measurement of urine proteinuria/creatinine ratios confirmed these findings. BP remained normal at all time points, and mean body weight at the end of follow up was comparable in both groups (Table 2).

MSC Treatment Reduces Loss of Glomeruli during Mesangiolytic Injury and Tubulointerstitial Fibrosis

On day 60, PAS-stained sections in all rats revealed glomeruli in various stages of repair or sclerosis besides very few glomeruli with relatively normal morphology (Figure 3, A and B). Approximately 20% of the glomeruli in MSC-treated rats exhibited large, "empty" defects of varying size. Adhesions between the glomerular tuft and Bowman's capsule occurred at similar frequencies (approximately 60%) in the two groups (data not shown). MSC treatment led to better preservation of glomeruli after the initial mesangiolytic injury, as evidenced by significantly more glomeruli per 1-mm^2 section of renal cortex (Figure 3C).

Focal tubulointerstitial injury was mildly reduced in the MSC group, but the difference to control rats failed to reach statistical significance (Figure 3D). However, tubulointerstitial collagen accumulation, as assessed by Sirius red staining, was significantly lower in the MSC group *versus* controls (Figure 3, E through G). Glomerular and tubulointerstitial infiltration by monocytes/macrophages did not differ between the groups on day 60 (data not shown).

MSC Treatment Leads to Persistent Mesangial Cell Activation on Day 60

Glomerular markers of mesangial cell activation (the *de novo* expression of α-SMA and interstitial collagen types [types I and III]) decreased by >50% between day 10 (Table 2) and day 60 (Figure 4, A through G). However, in MSC-treated rats on day 60, glomerular *de novo* expression of α-SMA (Figure 4, A through C), as well as the *de novo* expression of collagen type I (Figure 4, D through F) and type III (Figure 4G) and the constitutive expression of collagen type IV (Figure 4H) all were significantly increased as compared with the control group. In contrast, the expression of glomerular desmin, which is constitutively expressed by mesangial cells and *de novo* by activated podocytes, was not different between the groups (data not shown). Glomerular monocyte/macrophage counts were also not affected by MSC treatment on day 60 (data not shown).

Glomeruli of MSC-Treated Rats on Day 60 Contain Adipocytes

The most striking difference in PAS-stained sections between the two groups was the presence of very large singular or multiple defects that were devoid of any content and were exclusively observed in glomeruli (18.6 ± 7% of glomeruli),

Table 2. Functional and morphologic findings in nephritic, uninephrectomized rats on days 10, 30, and 60 after induction of anti-Thy1.1 nephritis and treatment with either intra-arterial injection of MSC or control medium into the left kidney on day 2[a]

Parameter	MSC Injection ($n = 10$[b])	Medium Injection ($n = 9$[b])	P
Day 10			
serum creatinine (μmol/L)	86 ± 15	125 ± 16	<0.001[c]
SUN (mmol/L)	16.4 ± 3.3	20.4 ± 2.9	<0.05[c]
creatinine clearance (ml/min)	0.43 ± 0.1	0.29 ± 0.1	<0.01
proteinuria (mg/d)	25 ± 7	32 ± 13	NS[c]
urine proteinuria/creatinine ratio	43 ± 14	49 ± 15	NS
SBP (mmHg)	131 ± 14	129 ± 9	NS
mesangiolysis score	1.05 ± 0.29	0.91 ± 0.34	NS
% of glomeruli with adhesions to Bowman's capsule	19.7 ± 9.8	36.5 ± 5.2	<0.01
mean ED-1–positive cells per glomerulus	5.6 ± 0.9	4.7 ± 1.5	NS
mitoses per 100 glomeruli	7.2 ± 2.4	8.4 ± 10	NS
glomerular α-SMA expression (% area stained positively)	30 ± 3	33 ± 6	NS
glomerular collagen type I expression (% area stained positively)	34 ± 3	29 ± 3	<0.05
Day 30			
serum creatinine (μmol/L)	54 ± 5	55 ± 4	NS[c]
SUN (mmol/L)	11.7 ± 1.4	13.6 ± 1.2	<0.05[d]
creatinine clearance (ml/min)	0.99 ± 0.2	0.99 ± 0.1	NS
proteinuria (mg/d)	13 ± 5	20 ± 9	<0.05[c]
urine proteinuria/creatinine ratio	15 ± 5	22 ± 10	NS ($P = 0.06$)
SBP (mmHg)	126 ± 8	126 ± 9	NS
Day 60			
serum creatinine (μmol/L)	61 ± 5	66 ± 5	NS[c]
creatinine clearance (ml/min)	1.09 ± 0.1	1.15 ± 0.2	NS
SUN (mmol/l)	12.4 ± 1.4	14.0 ± 1.3	<0.05[d]
proteinuria (mg/d)	13 ± 4	40 ± 25	<0.01[c]
urine proteinuria/creatinine ratio	12 ± 4	35 ± 25	<0.05
SBP (mmHg)	123 ± 10	117 ± 9	NS
body weight (g)	309 ± 18	315 ± 21	NS

[a] α-SMA, α-smooth muscle actin; MSC, mesenchymal stem cells; SBP, systolic BP; SUN, serum urea nitrogen.
[b] $n = 5$ each for the histologic analyses on day 10.
[c] P value confirmed using two-way repeated measures ANOVA.
[d] $P > 0.05$ (NS) using two-way repeated measures ANOVA.

exclusively in MSC-treated rats (Figure 5, A through H) and never on day 10 (Figure 6A) after disease induction. Most of these areas were surrounded by a zone of matrix accumulation that contained collagen types I, III, and IV plus α-SMA (Figure 5, C through F) as well as some monocytes/macrophages (Figure 5B). Within or adjacent to these areas, we frequently noted small cells with intense cellular staining for collagen types I and III (Figure 5, D and E, arrows) and Sirius red positivity (Figure 5H), which in serial sections failed to co-localize to ED-1–positive areas. Desmin expression in vacuolic areas was similar or less intense when compared with the rest of the glomerulus (Figure 5G). When examined by electron microscopy, the vacuoles were exclusively located intracellularly (Figure 5, I through K). Cells that contained individual large vacuoles as well as numerous small droplets strongly resembled the ultrastructural morphology of adipocytes. Even univacuolated cells, strongly resembling mature, signet-ring white adipocytes, were noted (Figure 5I). Oil red O staining confirmed that the cells contained lipids (triglycerides; Figure 5L), and Nile blue staining demonstrated the presence of neutral lipids (Figure 5M). In most cases, PKH26 fluorescence surrounded the nonfluorescent vacuolar areas (Figure 2C). In other cases, fluorescence was noted within fat vacuoles (Figure 2D).

We also asked which type of lipids are produced by MSC during adipogenic differentiation *in vitro*. As shown in Figure 5O, Nile blue staining confirmed the expression of neutral lipids, similar to the *in vivo* situation (Figure 5M).

Finally, we tried to assess whether adipogenic maldifferentiation may have started early during nephritis. On day 10 after disease induction (*i.e.*, 8 d after MSC injection), Oil red O

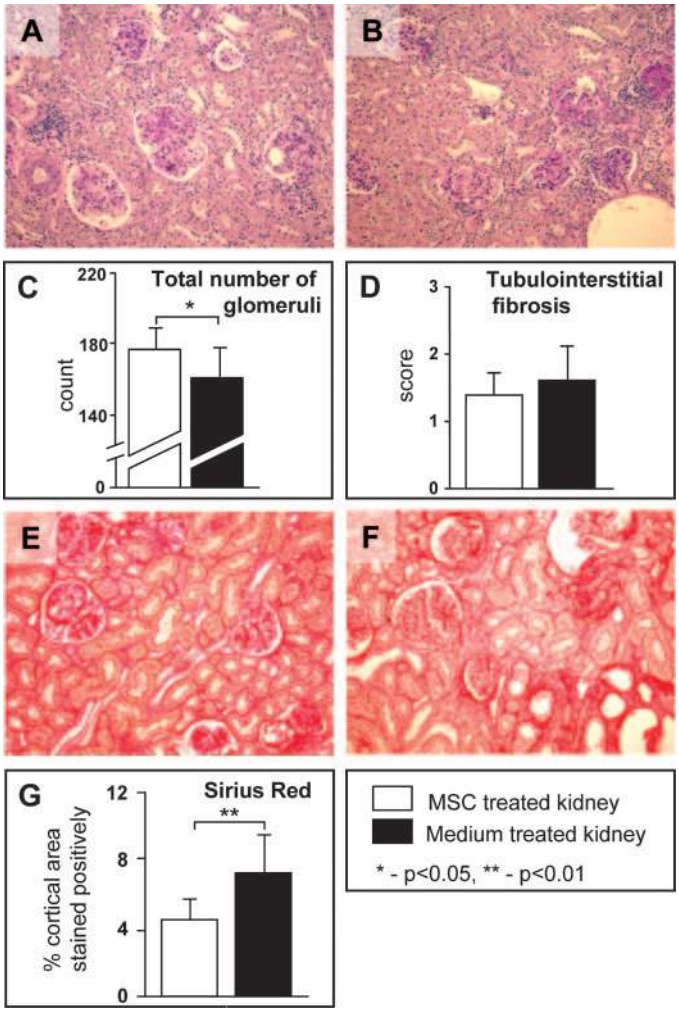

Figure 3. Overall histology and tubulointerstitial staining for Sirius red at day 60 after disease induction. Lewis rats that had anti-Thy1.1 nephritis and received MSC (A) or medium (B) into the left renal artery on day 2 after disease induction (periodic acid-Schiff [PAS] staining) with both exhibiting FSGS and glomerular adhesions of varying degrees. Quantification of total number of glomeruli (C) and cortical tubulointerstitial damage score (D). Sirius red staining in cortical tubulointerstitial areas of MSC-treated (E) *versus* medium-treated (F) rats and quantitative assessment (G). Magnification, ×100.

stainings (Figure 6C) and electron microscopy analyses (Figure 6, A and B) failed to detect intraglomerular fat cells. *In vitro* expression of typical fat cell markers (adiponectin, leptin, lipoprotein lipase, and peroxisome proliferator–activated receptor-γ) was low in undifferentiated MSC (passage 3), although higher than in mesangial cell controls. After 16 d of exposure to adipogenic induction medium and visible formation of fat cell clusters, the increase in expression of these markers was fivefold (leptin), 107-fold (peroxisome proliferator–activated receptor-γ), 248-fold (lipoprotein lipase), and 2572-fold (adiponectin; Figure 6D). We therefore conclude that the molecular profile of our cells before adipogenic differentiation differs substantially from that of differentiated adipocytes.

Discussion

In this study, we investigated long-term effects of intrarenal, syngeneic MSC transplantation in a progressive model of mesangioproliferative nephritis in rats. We chose medium injections for control rats because we showed previously that intrarenal injection of mesangial cells does not reproduce any of the MSC effects (6), which confirms observations of others (5), who used fibroblasts as control cells for intra-arterial MSC in a rat model of ARF.

The first major finding was that MSC in our aggravated model of anti-Thy1.1 nephritis potently ameliorated early ARF, which confirms our own and others' recent data in a less severe variant of this model (6,16). This effect likely resulted from paracrine effects of the transplanted MSC (6), leading to the reduction in glomerular adhesion formation and better long-term preservation of glomeruli observed in this study. As has been described before (4,5,6,17), MSC secrete high concentrations of growth factors such as VEGF, TGF-β, and hepatocyte growth factor. In particular, proangiogenic effects of VEGF (16) might help to restitute glomerular capillaries better. In contrast, we (6) and others (5) failed to detect any evidence of transdifferentiation of MSC into glomerular, tubular, or renal interstitial cells. Therefore, the reduction of tubulointerstitial fibrosis that was observed in our MSC-treated rats likely was a secondary effect, related to the better preservation of glomeruli. Functionally, our early MSC treatment led to a marginally better renal function on day 60 and prevented the progressive increase in proteinuria, consistent with better preservation of glomeruli.

The second major finding of our study was that on day 60, approximately 20% of the MSC-treated glomeruli contained cells that exhibited typical features of adipocytes. It seems highly likely that these originated from the transplanted MSC for several reasons: (*1*) Similar cells were never observed in the control group; (*2*) in a multitude of spontaneous or induced models of glomerular disease as well as in human glomerular disease, we never observed glomerular adipocytes; (*3*) lipid characterization yielded similar findings in the adipocytes *in vivo* and in MSC that underwent adipogenic differentiation *in vitro*; and (*4*) the adipocytes were almost always surrounded by intense PKH26-specific fluorescence or the lipid even contained it. Nevertheless, this does not allow us to count distinct MSC offspring. Some areas exhibited diffuse and weak PKH26 fluorescence, and several phenomena may underlie the staining pattern, including (*1*) MSC division and thereby dilution of the dye, (*2*) cell death and uptake of the dye by neighboring cells, and (*3*) diffusion of the dye into the lipid droplets.

Are the adipocytes indeed derived from MSC or from other bone marrow cells that contaminated the preparation? Despite culture under particular conditions before transplantation of the MSC, the latter cannot be formally excluded, because no specific MSC markers are available. However, on the basis of recommendations of a consensus paper on MSC characterization (15), our cells fully matched the consensus requirements. To rule out a contamination of the injected cells by adipocytes, we first showed that nephritic, MSC-injected kidneys on day 10 showed no signs of adipocyte formation or accidental adipo-

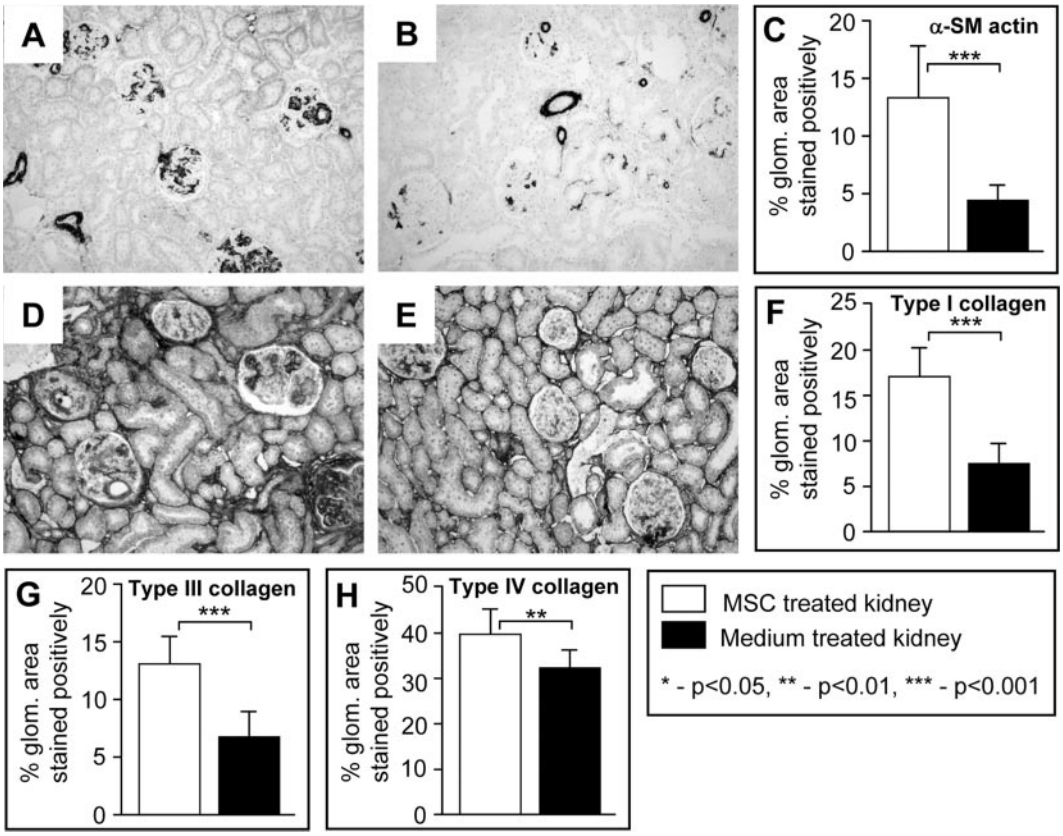

Figure 4. Glomerular α-smooth muscle actin (α-SMA) expression (A through C) and matrix deposition (D through H) in Lewis rats that had anti-Thy1.1 nephritis and received MSC (A and D) or medium (B and E) into the left renal artery on day 2 after disease induction and quantitative analyses of renal histologic changes at day 60. Magnification, ×100.

cyte transplantation. Furthermore, before and after induction of adipogenic MSC differentiation, we noted an up to 2500-fold increase of adipocyte markers. This renders it very unlikely that our cell cultures might have been contaminated by significant numbers of mature adipocytes or even preadipocytes. Another possible explanation is adipocyte formation as a result of intrinsic glomerular cells' reacting to neighboring MSC. This cannot be formally excluded because of the given technical limitations of long-term cell tracking, but we want to stress that no other condition in which glomerular cells differentiate to adipocytes *in vivo* or *in vitro* is known.

Glomerular adipocyte formation in MSC-treated rats was accompanied by a pronounced fibrotic response, which may largely account for the highly significant increase in glomerular deposition of collagen types I, III, and IV and the smooth muscle cell marker α-SMA on day 60 (Figure 4). Whether this fibrotic wall, in particular the small cells that were very intensely positive for collagens type I and III and directly adjacent to the adipocytes, derived from activated mesangial cells or MSC is unknown, because both can express collagen types I and III (18,19). MSC-derived adipocytes may contribute to a fibrotic response *via* mechanic stretch or through their proinflammatory activity (20,21). Our data resemble findings that were obtained in the lung, where murine MSC were trapped, and formed cysts with adjacent collagen depositions, resulting in severe lung damage (22).

Despite the apparent maldifferentiation of glomerular MSC into adipocytes and the fibrotic response surrounding them, which might have decreased GFR, renal function on day 60 after disease induction, if at all, was better preserved than that of controls. This is likely the consequence of two counteracting effects of MSC treatment: Improved early preservation of glomeruli during mesangiolysis on the one hand and maldifferentiation and fibrosis in approximately 20% of glomeruli on the other hand. Whether a similar mutual neutralization of beneficial and adverse effects would also occur in other models remains to be determined. However, the morphologic aspect of glomeruli that contain adipocytes strongly suggests that these glomeruli should exhibit a marked functional impairment and ultimately develop global glomerulosclerosis.

MSC have the ability to differentiate into new phenotypes along particular mesenchymal lineages in response to various microenvironments (23). Mesenchymal differentiation includes adipocytes, osteocytes, and chondrocytes, but MSC plasticity can also lead to "unorthodox" differentiation toward hepatocytes, (24), cardiomyocytes (25), and neural cells (26). Whether "orthodox" or "unorthodox" differentiation, it is always expected to take place in the appropriate environment and to the benefit of the individual. Here we show for the first time "orthodox" differentiation of MSC into fat cells but in an inappropriate, "unorthodox" location.

Why did our MSC differentiate into adipocytes but not os-

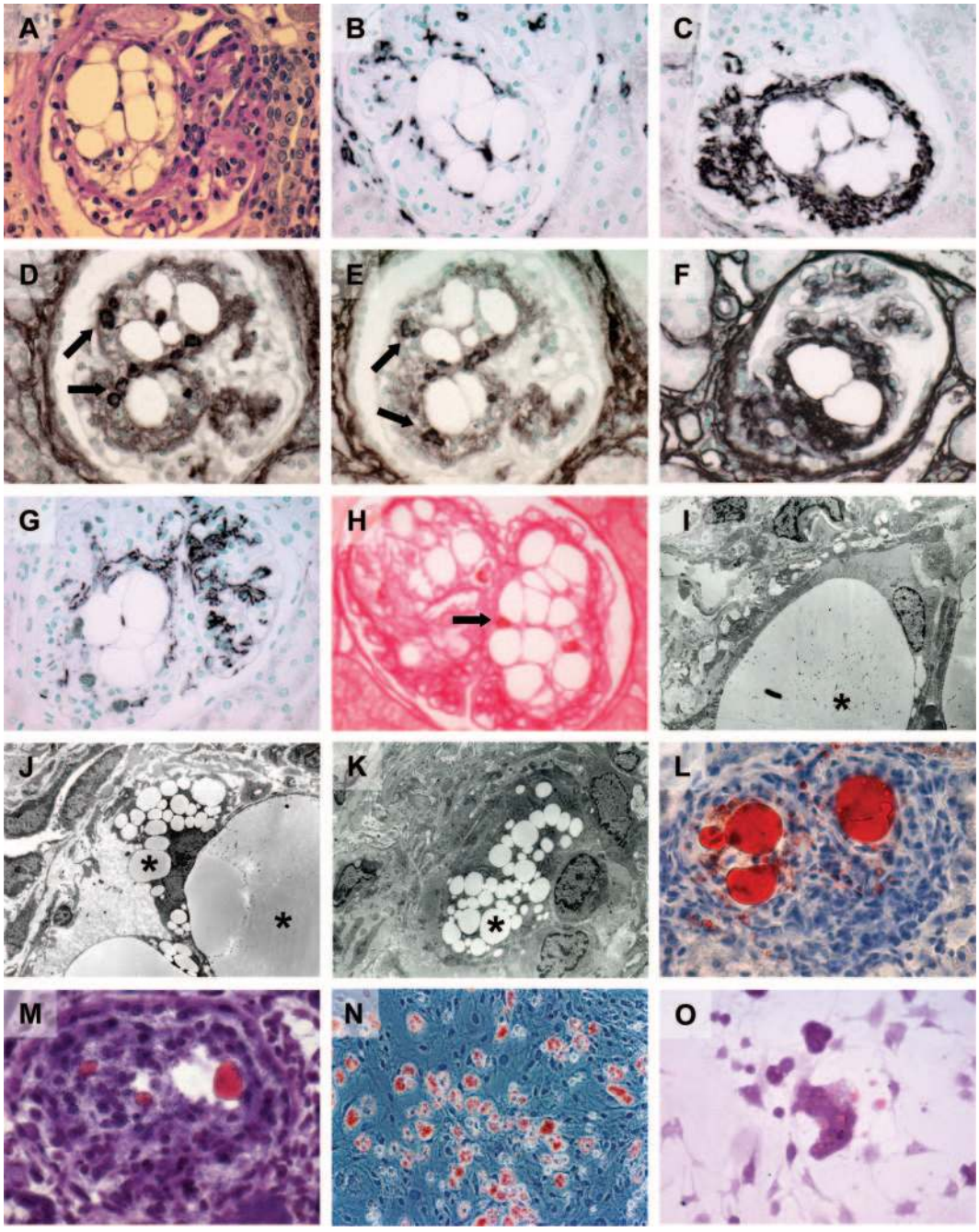

Figure 5. Morphology of adipocytes in MSC-treated Lewis rats with anti-Thy1.1 nephritis on day 60. (A) PAS staining shows "vacuolar" glomerular changes. (B) Staining for ED-1 shows monocytes/macrophages surrounding the vacuoles. (C) Staining for α-SMA shows an intense reaction surrounding the vacuoles. (D) Staining for collagen type I exhibiting several strongly stained small cells (arrows) located in close proximity to the vacuoles. These cells are also detected by immunostaining for collagen type III (E, serial section, arrows). (F) Staining for collagen type IV similarly shows an intense fibrotic response surrounding the vacuole. (G) Expression of glomerular desmin is not enhanced in the vicinity of the vacuoles. (H) Sirius red staining for overall collagen deposition. Again, small cells with intense staining (arrows) are distinguishable in association with fat vacuoles. (I through K) Electron microscopy images of vacuolic areas (*) demonstrating their intracellular location. The figures demonstrate adipocytes with large or multiple small fatty vacuoles and perfectly match the histochemical results. (L) Oil red O staining showing intraglomerular areas with densely packed triglycerides (red color) located inside a vacuolic area. (M) staining with Nile blue showed the intraglomerular fat vacuoles to be composed of neutral lipids (pink color). (N and O) Lewis MSC that were cultured for 15 d with complete medium after induction with adipogenic supplements. (N) Cells *in vitro* showing accumulation of lipid-rich, Oil red O–positive vacuoles). (O) Nile blue staining shows pink lipid vacuoles indicating neutral lipids. Magnifications: ×400 in A through G, L, M; ×2800 in I through K; ×200 in N and O.

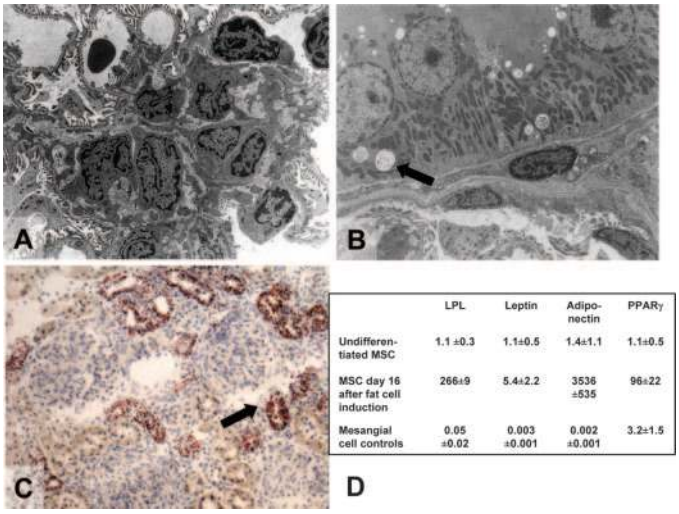

	LPL	Leptin	Adipo-nectin	PPARγ
Undifferen-tiated MSC	1.1 ±0.3	1.1±0.5	1.4±1.1	1.1±0.5
MSC day 16 after fat cell induction	266±9	5.4±2.2	3536 ±535	96±22
Mesangial cell controls	0.05 ±0.02	0.003 ±0.001	0.002 ±0.001	3.2±1.5

Figure 6. Assessment of early adipocytic markers. Electron microscopy pictures of MSC-treated Lewis rats on day 10 after disease induction. (A) No evidence of intraglomerular adipocytes. (B) As opposed to glomerular cells, tubular cells show inclusion of lipid droplets (arrow), a phenomenon that is correlated with significant proteinuria. (C) Oil red O staining at day 10 confirmed these findings. (D) Molecular upregulation of adipocyte markers 16 d after induction of fat cell differentiation. mRNA expression relative to the mean of undifferentiated MSC. LPL, lipoprotein lipase. Magnifications: ×5000 in A and B; ×200 in C.

teocytes or chondrocytes? At least in the case of chondrogenic differentiation, stem cells *in vivo* have to be pelleted to form a micromass and have to be cultured as such. A glomerulus therefore may not provide adequate physical conditions for chondrogenic differentiation. Rather, TGF-β, which is secreted in high amounts by our MSC *in vitro* (6), acts as a major signal for adipogenesis (27,28). Another factor that strongly enhances adipogenic differentiation of MSC *in vitro* is basic fibroblast growth factor (29), which is released within the glomerulus during early anti-Thy1.1 nephritis (30). Finally, human adipocytes express Fc receptors, and lipogenesis is stimulated by Ig as efficiently as by insulin (20). Elevated Ig levels during anti-Thy1.1 nephritis therefore could contribute to adipogenesis.

Others have experienced unwanted, stem cell–associated phenomena as well. Wu *et al.* (31) showed fibroblast-like differentiation of MSC in the setting of chronic heart allograft rejection. Toegel *et al.* (32) reported the formation of unique "proximal tubular pseudocrescents" in the glomeruli of mice after mobilization of hematopoietic stem cells with cyclophosphamide and G-CSF before induction of acute ischemic renal failure. However, in that study, it remained unclear whether stem cells contributed to this phenomenon, because pseudocrescents were very rarely noted in control groups as well. Finally, stem cells can contribute to malignancy, for example, *via* teratoma formation after injection of embryonic stem cells (33), in *Helicobacter*-associated gastric cancer (34), or by tumor-associated myofibroblasts and fibroblasts (35).

Others (36,37) have studied the contribution of either normal or intravenously infused bone marrow to the regeneration of damaged glomeruli in a rat model similar to ours. It was found that bone marrow mainly contributed to glomerular endothelial cell regeneration, and infused bone marrow prevented death of nephritic animals in the study of Li *et al.* (37). In both studies, no intraglomerular adipocytes were noted after 11 to 12 wk, again suggesting that intraglomerular adipogenesis in our study does not happen during the normal course of the disease model but must be linked directly to intraglomerular injection of MSC. Given this, our findings are in line with the new ecological concept of the stem cell niche (38).

Our novel observation of "orthodox MSC differentiation" in an "unorthodox location" raises considerable concerns about the safety of MSC-based cell therapies. Resolving these concerns will require extensive tests to evaluate how to prevent such unwanted differentiation. For example, in the case of MSC, preincubation with PDGF-B or retinoid acid induced a mesangial cell–like phenotype *in vitro* (39). Alternatively, other sources for MSC might be used: Kern *et al.* (40) showed that MSC from bone marrow or adipose tissue but not those from umbilical cord blood can differentiate into adipocytes. Prolonged *ex vivo* expansion of human MSC and senescence itself led to a loss of adipogenic differentiation potential and therefore might render MSC less susceptible to maldifferentiation *in vivo* (41).

Acknowledgments

This work was supported by a grant from the "Interdisciplinary Center for Clinical Research in Biomaterials and Tissue-Material-Interaction in Implants" (IZKF BIOMAT of the RWTH Aachen) and a "Lise-Meitner" stipend of the state North-Rhine Westfalia to U.K. as well as by a grant from the German Research Foundation (SFB 542, C7) to J.F. and T.O. and a stipend from the International Society of Nephrology to Z.D. and M.M.-P.

The help of Gabi Dietzel, Andrea Cosler, Gerti Minnartz, and Katrin Haerthel is gratefully acknowledged.

Disclosures

None.

References

1. Anglani F, Forino M, Del Prete D, Tosetto E, Torregrossa R, D'Angelo A: In search of adult renal stem cells. *J Cell Mol Med* 4: 474–487, 2004
2. Herrera MB, Bussolati B, Bruno S, Fonsato V, Romanazzi GM, Camussi G: Mesenchymal stem cells contribute to the renal repair of acute tubular epithelial injury. *Int J Mol Med* 14: 1035–1041, 2004
3. Morigi M, Imberti B, Zoja C, Corna D, Tomasoni S, Abbate M, Rottoli D, Angioletti S, Benigni A, Perico N, Alison M, Remuzzi G: Mesenchymal stem cells are renotropic, helping to repair the kidney and improve function in acute renal failure. *J Am Soc Nephrol* 15: 1794–1804, 2004
4. Lange C, Togel F, Ittrich H, Clayton F, Nolte-Ernsting C, Zander AR, Westenfelder C: Administered mesenchymal stem cells enhance recovery from ischemia/reperfusion-induced acute renal failure in rats. *Kindey Int* 68: 1613–1617, 2005

5. Togel F, Hu Z, Weiss K, Isaac J, Lange C, Westenfelder C: Administered mesenchymal stem cells protect against ischemic acute renal failure through differentiation-independent mechanisms. *Am J Physiol Renal Physiol* 289: F29–F30, 2005
6. Kunter U, Rong S, Djuric Z, Boor P, Muller-Newen G, Yu D, Floege J: Transplanted mesenchymal stem cells accelerate glomerular healing in experimental glomerulonephritis. *J Am Soc Nephrol* 17: 2202–2212, 2006
7. Kriz W, Hahnel B, Hosser H, Ostendorf T, Gaertner S, Kranzlin B, Gretz N, Shimizu F, Floege J: Pathways to recovery and loss of nephrons in anti-Thy-1 nephritis. *J Am Soc Nephrol* 14: 1904–1926, 2003
8. Ostendorf T, Rong S, Boor P, Wiedemann S, Kunter U, Haubold U, van Roeyen CRC, Eitner F, Kawachi H, Starling G, Alvarez E, Smithson G, Floege J: Antagonism of PDGF-D by human antibody CR002 prevents renal scarring in experimental glomerulonephritis. *J Am Soc Nephrol* 17: 1054–1062, 2006
9. van Roeyen CR, Ostendorf T, Denecke B, Bokemeyer D, Behrmann I, Strutz F, Lichenstein HS, LaRochelle WJ, Pena CE, Chaudhuri A, Floege J: Biological responses to PDGF-BB versus PDGF-DD in human mesangial cells. *Kidney Int* 69: 1393–1402, 2006
10. Ostendorf T, Kunter U, Eitner F, Loos A, Regele H, Kerjaschki D, Henninger DD, Janjic N, Floege J: VEGF 165 mediates glomerular endothelial repair. *J Clin Invest* 104: 913–923, 1999
11. Burg M, Ostendorf T, Mooney A, Koch KM, Floege J: Treatment of experimental mesangioproliferative glomerulonephritis with non-anticoagulant heparin: Therapeutic efficacy and safety. *Lab Invest* 76: 505–516, 1997
12. Yoshimura A, Gordon K, Alpers CE, Floege J, Pritzl P, Ross R, Couser WG, Bowen-Pope DF, Johnson RJ: Demonstration of PDGF B-chain mRNA in glomeruli in mesangial proliferative nephritis by in situ hybridization. *Kidney Int* 40: 470–476, 1991
13. Floege J, Hackmann B, Kliem V, Kriz W, Alpers CE, Johnson RJ, Kuhn KW, Koch KM, Brunkhorst R: Age-related glomerulosclerosis and interstitial fibrosis in Milan normotensive rats: A podocyte disease. *Kidney Int* 51: 230–243, 1997
14. Ostendorf T, Kunter U, Grone HJ, Bahlmann F, Kawachi H, Shimizu F, Koch KM, Janjic N, Floege J: Specific antagonism of PDGF prevents renal scarring in experimental glomerulonephritis. *J Am Soc Nephrol* 12: 909–918, 2001
15. Dominici M, Le Blanc K, Mueller I, Slaper-Cortenbach I, Marini FC, Krause DS, Deans RJ, Keating A, Prockop DJ, Horwitz EM: Minimal criteria for defining multipotent mesenchymal stromal cells. The International Society for Cellular Therapy position statement. *Cytotherapy* 8: 315–317, 2006
16. Uchimura H, Marumo T, Takase O, Kawachi H, Shimizu F, Hayashi M, Saruta T, Hishikawa K, Fujita T: Intrarenal injection of bone marrow-derived angiogenic cells reduces endothelial injury and mesangial cell activation in experimental glomerulonephritis. *J Am Soc Nephrol* 16: 997–1004, 2005
17. Kinnaird T, Stabile E, Burnett MS, Lee CW, Barr S, Fuchs S, Epstein SE: Marrow-derived stromal cells express genes encoding a broad spectrum of arteriogenic cytokines and promote in vitro and in vivo arteriogenesis through paracrine mechanisms. *Circ Res* 94: 678–685, 2004
18. Gouttenoire J, Valcourt U, Ronziere MC, Aubert-Foucher E, Mallein-Gerin F, Herbage D: Modulation of collagen synthesis in normal and osteoarthritic cartilage. *Biorheology* 41: 535–542, 2004
19. Franz-Odendaal TA, Hall BK, Witten PE: Buried alive: How osteoblasts become osteocytes. *Dev Dyn* 235: 176–190, 2006
20. Palming J, Gabrielsson BG, Jennische E, Smith U, Carlsson B, Carlsson LM, Lonn M: Plasma cells and Fc receptors in human adipose tissue: Lipogenic and anti-inflammatory effects of immunoglobulins on adipocytes. *Biochem Biophys Res Commun* 343: 43–48, 2006
21. Neels JG, Olefsky JM: Inflamed fat: What starts the fire? *J Clin Invest* 116: 33–35, 2006
22. Anjos-Afonso F, Siapati EK, Bonnet D: In vivo contribution of murine mesenchymal stem cells into multiple cell-types under minimal damage conditions. *J Cell Sci* 117: 5655–5664, 2004
23. Pittenger MF, Mackay AM, Beck SC, Jaiswal RK, Douglas R, Mosca JD, Moormann MA, Simonetti DW, Craig S, Marshak DR: Multilineage potential of adult mesenchymal stem cells. *Science* 284: 143–147, 1999
24. Sato Y, Araki H, Kato J, Nakamura K, Kawano Y, Kobune M, Sato T, Miyanishi K, Takayama T, Takahashi M, Takimoto R, Iyama S, Matsunaga T, Ohtani S, Matsuura A, Hamada H, Niitsu Y: Human mesenchymal stem cells xenografted directly to rat liver are differentiated into human hepatocytes without fusion. *Blood* 106: 756–763, 2005
25. Fukuda K: Development of regenerative cardiomyocytes from mesenchymal stem cells for cardiovascular tissue engineering. *Artif Organs* 25: 187–193, 2001
26. Sanchez-Ramos J, Song S, Cardozo-Pelaez F, Hazzi C, Stedeford T, Willing A, Freeman TB, Saporta S, Janssen W, Patel N, Cooper DR, Sanberg PR: Adult bone marrow stromal cells differentiate into neural cells in vitro. *Exp Neurol* 164: 247–256, 2000
27. Teruel T, Valverde AM, Benito M, Lorenzo M: Transforming growth factor beta 1 induces differentiation-specific gene expression in fetal rat brown adipocytes. *FEBS Lett* 364: 193–197, 1995
28. Ahdjoudji S, Lasmoles F, Holy X, Zerath E, Marie PJ: Transforming growth factor beta2 inhibits adipocyte differentiation induced by skeletal unloading in rat bone marrow stroma. *J Bone Miner Res* 17: 668–677, 2002
29. Neubauer M, Fischbach C, Bauer-Kreisel P, Lieb E, Hacker M, Tessmar J, Schulz MB, Goepferich A, Blunk T: Basic fibroblast growth factor enhances PPARgamma ligand-induced adipogenesis of mesenchymal stem cells. *FEBS Lett* 577: 277–283, 2004
30. Floege J, Eng E, Lindner V, Alpers CE, Young BA, Reidy MA, Johnson RJ: Rat glomerular mesangial cells synthesize basic fibroblast growth factor. Release, upregulated synthesis, and mitogenicity in mesangial proliferative glomerulonephritis. *J Clin Invest* 90: 2362–2369, 1992
31. Wu GD, Nolta JA, Jin YS, Baar ML, Yu H, Starnes VA, Cramer DV: Migration of mesenchymal stem cells to heart allografts during chronic rejection. *Transplantation* 75: 679–685, 2003
32. Togel F, Isaac J, Westenfelder C: Hematopoietic stem cell

mobilization-associated granulocytosis severely worsens acute renal failure. *J Am Soc Nephrol* 15: 1261–1267, 2004
33. Thomson JA, Itskovitz-Eldor J, Shapiro SS, Waknitz MA, Swiergiel JJ, Marshall VS, Jones JM: Embryonic stem cell lines derived from human blastocysts. *Science* 282: 1145–1147, 1998
34. Houghton JM, Stoicov C, Nomura S, Rogers AB, Carlson J, Li H, Cai X, Fox JG, Goldenring JR, Wang TC: Gastric cancer originating from bone marrow-derived cells. *Science* 306: 1568–1571, 2004
35. Direkze NC, Hodivala-Dilke K, Jeffery R, Hunt T, Poulsom R, Oukrif D, Alison MR, Wright NA: Bone marrow contribution to tumor-associated myofibroblasts and fibroblasts. *Cancer Res* 64: 8492–8495, 2004
36. Ikarashi K, Li B, Suwa M, Kawamura K, Morioka T, Yao J, Khan F, Uchiyama M, Oite T: Bone marrow cells contribute to regeneration of damaged glomerular endothelial cells. *Kidney Int* 67: 1925–1933, 2005
37. Li B, Morioka T, Uchiyama M, Oite T: Bone marrow cell infusion ameliorates progressive glomerulosclerosis in an experimental rat model. *Kidney Int* 69: 323–330, 2006
38. Powell K: Stem-cell niches: It's the ecology, stupid! *Nature* 435: 268–270, 2005
39. Suzuki A, Iwatani H, Ita T, Imai E, Okabe M, Nakamura H, Isaka Y, Yamato M, Hori M: Platelet-derived growth factor plays a critical role to convert bone marrow cells into glomerular mesangial-like cells. *Kidney Int* 65: 15–24, 2004
40. Kern S, Eichler H, Stoeve J, Kluter H, Bieback K: Comparative analysis of mesenchymal stem cells from bone marrow, umbilical cord blood or adipose tissue. *Stem Cells* 24: 1294–1301, 2006
41. Mauney JR, Volloch V, Kaplan DL: Matrix-mediated retention of adipogenic differentiation potential by human adult bone marrow-derived mesenchymal stem cells during ex vivo expansion. *Biomaterials* 26: 6167–6175, 2005